Spin-orbit interactions between interchain excitations in conjugated polymers

William Barford,[1,*] Robert J. Bursill,[2,†] and Dmitry V. Makhov[1,‡]
[1]*Department of Chemistry, Physical and Theoretical Chemistry Laboratory, University of Oxford, Oxford OX1 3QZ, United Kingdom*
[2]*School of Physics, University of New South Wales, Sydney, New South Wales 2052, Australia*
(Received 2 November 2009; revised manuscript received 22 December 2009; published 20 January 2010)

Motivated by the reported enhanced singlet exciton yield in light-emitting polymers, we investigate spin-orbit coupling between Coulombically bound interchain excitations. We show theoretically that because of the close similarity of the singlet and triplet interchain wave functions, spin-orbit coupling between these states is negligible. Using density matrix renormalization group calculations on model systems, we confirm these theoretical predictions: spin-orbit coupling between interchain states is typically 10^3-10^4 times smaller than between corresponding intramolecular states, being typically ca. 1×10^{-7} eV for disordered polymers. We discuss the implication of these results for the possibly enhanced singlet exciton yield in light-emitting polymers.

DOI: 10.1103/PhysRevB.81.035206 PACS number(s): 71.70.Ej, 71.35.−y, 71.20.Rv

I. INTRODUCTION

One of the factors that determines the internal electroluminescent quantum efficiency of polymer light-emitting devices is the yield of singlet excitons formed by the recombination of the injected electrons and holes. Singlet exciton yields in light-emitting polymers exceeding the spin-independent recombination value of 25% has been reported by a large number of groups,[1–7] although its value remains highly controversial.[8]

Various theoretical models have been proposed to explain the possible enhanced singlet yield. All of these models propose a long-lived intermediate triplet state that either undergoes intersystem crossing (ISC) to a singlet state or decays to a lower-lying triplet state. Refs. 9–11 propose an intramolecular intermediate triplet state that interconverts to other intramolecular states. References 12–15, on the other hand, propose an intermolecular intermediate triplet state that either intersystem crosses to a short-lived intermolecular singlet (which rapidly interconverts to an intramolecular state) or interconverts directly to an intramolecular triplet state. Barford[15] also proposed selection rules that apply to well-ordered systems, which inhibit certain intermolecular interconversion processes, implying that the large intramolecular singlet-triplet exchange gap strongly inhibits the triplet interconversion process.

Having established the theoretical possibility of long-lived intermediate triplets, the remaining issue is whether there are any ISC mechanisms with rates comparable to or faster than the triplet interconversion rate. In this paper we consider spin-orbit coupling as a possible mechanism for ISC between Coulombically bound interchain singlet and triplet states. We show that for such interchain excitations spin-orbit coupling is negligible and cannot compete with intermolecular interconversion rates. This conclusion is in agreement with the experimental observations of Reufer *et al.*[16]

There are two well-known reasons why ISC rates are small for conjugated polymers in general,[17,18] and a third reason why they are especially small between quasidegenerate interchain excitations in particular. The two general reasons are that for π-electron systems, the effective nuclear charge is small and the spin-orbit coupling matrix elements vanish between π orbitals in planar systems. The third reason that is particular to interchain excitations is due to the property that the spin-orbit matrix elements between a pair of states are proportional to the differences in their spatial wave functions. For the quasidegenerate interchain excitations of relevance in this work, these differences are small, and consequently the spin-orbit matrix elements are also very small. (Calculated spin-orbit coupling matrix elements in conjugated polymers between intramolecular excitons[19] and single polarons[20] have recently been reported in the literature.)

In the next section these points are explained in more detail. It will be shown that the physical characteristics of interchain excitations are crucial to our discussion, so Sec. III is devoted to a description of these states. We use density matrix renormalization calculations on model systems to confirm our theoretical considerations. We make concluding comments in Sec. IV

II. PROOFS THAT SPIN-ORBIT COUPLING IS NEGLIGIBLE FOR REAL SYSTEMS AND VANISHING FOR IDEAL π-ELECTRON SYSTEMS

A. Spin-orbit coupling of π electrons

The one-electron spin-orbit operator is

$$\hat{H}_{SO}=\sum_{i}^{N}\hat{H}_{SO}^{(i)} \tag{1}$$

where

$$\hat{H}_{SO}^{(i)}=\alpha^2\sum_{n}^{N}\frac{Z_n}{R_{ni}^3}\hat{\mathbf{L}}_i^{(n)}\cdot\hat{\mathbf{S}}_i, \tag{2}$$

the sum i is over electrons, the sum n is over nuclei, and R_{ni} is the distance between the nth nucleus and the ith electron. $\hat{\mathbf{L}}_i^{(n)}$ is the angular momentum operator for the ith electron associated with the nth nucleus, α is the fine structure constant $(=7.297\cdots\times10^{-3})$, and Z_n is the effective nuclear charge.

In general we require atomic spin-orbital matrix elements of the form

$$\langle \alpha'^{(n')}, \sigma' | \sum_{n''}^{N} \frac{Z_{n''}}{R_{n''}^3} \hat{\mathbf{L}}^{(n'')} . \hat{\mathbf{S}} | \alpha^{(n)}, \sigma \rangle, \tag{3}$$

where $|\alpha^{(n)}, \sigma\rangle$ is an atomic spin-orbital of type α and spin σ localized on atom n. Let us suppose that n and n' are the same or neighboring carbon atoms. Let us further suppose that we may restrict the sum over atoms in Eq. (3) to the carbon atom containing orbital $|\alpha^{(n)}\rangle$ and the neighboring carbon atom. Then, using the Hermitian properties of $\hat{H}_{SO}^{(i)}$ the matrix elements take the form

$$\langle \alpha'^{(n')}, \sigma' | \frac{Z_n}{R_n^3} \hat{\mathbf{L}}^{(n)} . \hat{\mathbf{S}} | \alpha^{(n)}, \sigma \rangle, \tag{4}$$

where the operator $\hat{\mathbf{L}}^{(n)}.\hat{\mathbf{S}}$ acts on the orbital localized on atom n.

Now, in the spin-orbital basis $\{|2s,\uparrow\rangle, |2s,\downarrow\rangle, |2p_x,\uparrow\rangle, |2p_x,\downarrow\rangle, |2p_y,\uparrow\rangle, |2p_y,\downarrow\rangle, |2p_z,\uparrow\rangle, |2p_z,\downarrow\rangle\}$ the matrix of the operator $\hat{\mathbf{L}}\cdot\hat{\mathbf{S}}$ is

$$\hat{\mathbf{L}}\cdot\hat{\mathbf{S}} = \frac{i}{2}\begin{pmatrix} \mathbf{0} & \mathbf{0} & \mathbf{0} & \mathbf{0} \\ \mathbf{0} & \mathbf{0} & \begin{matrix} -1 & 0 \\ 0 & +1 \end{matrix} & \begin{matrix} 0 & -i \\ +i & 0 \end{matrix} \\ \mathbf{0} & \begin{matrix} +1 & 0 \\ 0 & -1 \end{matrix} & \mathbf{0} & \begin{matrix} 0 & -1 \\ -1 & 0 \end{matrix} \\ \mathbf{0} & \begin{matrix} 0 & +i \\ -i & 0 \end{matrix} & \begin{matrix} 0 & +1 \\ +1 & 0 \end{matrix} & \mathbf{0} \end{pmatrix}, \tag{5}$$

where $\mathbf{0}=\left(\begin{smallmatrix} 0 & 0 \\ 0 & 0 \end{smallmatrix}\right)$.

From Eq. (5) we observe that

$$\hat{\mathbf{L}}\cdot\hat{\mathbf{S}}|2p_z,\sigma\rangle = \frac{i}{2}(i|2p_x,\bar{\sigma}\rangle \mathrm{sgn}(\sigma) - |2p_y,\bar{\sigma}\rangle). \tag{6}$$

Thus, the operator $\hat{\mathbf{L}}\cdot\hat{\mathbf{S}}$ changes both the orbital and spin angular momentum projections of a π electron. For π-electron systems this implies that:

(1) The spin-orbit coupling connects singlet excitons with $S_z=\pm 1$ triplet excitons;[11]

(2) The matrix elements of $\hat{\mathbf{L}}\cdot\hat{\mathbf{S}}$ are nonzero only if the local axis of quantization rotates between neighboring atoms. In particular, for a spiral along the bond between two carbon atoms (defined by the x axis) the matrix elements are proportional to sin θ, where θ is the twist angle.[11,20]

The spin-orbit coupling matrix element between neighboring π orbitals is therefore[21]

$$A = B \sin\theta, \tag{7}$$

where

$$B = -i\frac{Z_n\alpha^2}{2}\langle p_z^{(n+1)}|R_n^{-3}|p_z^{(n)}\rangle \tag{8}$$

(in atomic units). Taking the effective charge $Z_n=4$ for π electrons (i.e., assuming full screening from the $1s$ electrons), and using Slater orbitals with a bond length of 1.4 Å we calculate $|B|=3.94\times10^{-4}$ eV.

B. Symmetry restrictions on spin-orbit coupling

We now consider the symmetry restrictions on spin-orbit coupling in π-electron systems implied by the results described in Sec. II A. The pure-imaginary Hermitian properties of the angular momentum operator imply that $\langle \alpha'^{(n')}|\hat{L}|\alpha^{(n)}\rangle \equiv -\langle \alpha^{(n)}|\hat{L}|\alpha'^{(n')}\rangle$, and so the relevant one-electron spin-orbit operator that connects singlet states with $S_z=1$ triplet states is now expressed in second quantized formalism as

$$\hat{H}_{SO} = \sum_{n}^{N-1} A(\hat{c}_{n\uparrow}^{\dagger}\hat{c}_{n+1\downarrow} - \hat{c}_{n+1\uparrow}^{\dagger}\hat{c}_{n\downarrow}), \tag{9}$$

where $\hat{c}_{n\sigma}^{\dagger}$ ($\hat{c}_{n\sigma}$) creates (destroys) a π electron on site n and A is defined by Eqs. (7) and (8).

We note in general that $\hat{H}_{SO}$ does not transform as the totally symmetric spatial irreducible representation, and thus for systems with a definite point group symmetry it will not connect states with the same spatial symmetry.[17]

In the next section we consider model systems with the following spatial symmetries (as illustrated in Fig. 3):

(1) Calculation 1: Perfectly co-planar molecules with no longitudinal displacement, belonging to the D_{2h} point group. Defining the molecular axis as the x axis and the axis normal to the repeat units as the z axis, in this point group H_{SO} transforms as B_{3u}, i.e., as x.

(2) Calculation 2: Co-planar molecules with a relative longitudinal displacement, belonging to the C_{2h} point group. In this point group H_{SO} transforms as B_u.

Although idealized, the alternating long and short bonds of these structures mean that they capture the key physics of conjugated polymers. Finally, we note that H_{SO} is odd under the particle-hole transformation $\hat{c}_{i\sigma}^{\dagger}\rightarrow(-1)^i\hat{c}_{i\bar{\sigma}}$. Since, where particle-hole symmetry is applicable, the lowest interchain singlet and triplet excitations have opposite particle-hole symmetry, it follows that there is no particle-hole symmetry restriction on ISC.

C. Spin-orbit operator couples states with different spatial wave functions

The pure-imaginary Hermitian properties of the angular momentum operator imply that its diagonal matrix elements vanish within a space of real spatial wave functions. Thus, if the total singlet and triplet states are expressed as

$$|\Psi_S\rangle = |\psi_S\rangle|\phi_S\rangle \tag{10}$$

and

$$|\Psi_T\rangle = |\psi_T\rangle|\phi_T\rangle, \tag{11}$$

respectively, where $|\psi\rangle$ and $|\phi\rangle$ are the spatial and spin wave functions, then using the result that $\langle\psi|\hat{\mathbf{L}}|\psi\rangle=0$ when $|\psi\rangle$ is real it follows that

$$\langle\Psi_S|\hat{\mathbf{L}}\cdot\hat{\mathbf{S}}|\Psi_T\rangle = \langle\psi_S|\hat{\mathbf{L}}|\Delta\psi\rangle\cdot\langle\phi_S|\hat{\mathbf{S}}|\phi_T\rangle, \tag{12}$$

where

$$|\Delta\psi\rangle = |\psi_S\rangle - |\psi_T\rangle. \tag{13}$$

Now, as shown in more detail in Sec. III A, neglecting direct exchange processes, to zeroth order in the intermolecular interactions, the singlet and triplet interchain excitations are equivalent (and degenerate). This degeneracy is lifted by intermolecular hybridization (or hopping) terms that exchange the spins. Denoting the energy scale for intermolecular hybridization by t_{inter}, to first order in t_{inter}, $|\Delta\psi\rangle$ is proportional to $t_{\text{inter}}/\Delta E$, where ΔE is the energy difference between the interchain states and relevant intrachain states, and in general $t_{\text{inter}} \ll \Delta E$. Thus, $|\Delta\psi\rangle$ and hence spin-orbit coupling vanishes as $t_{\text{inter}} \ll \Delta E$.

III. COULOMBICALLY BOUND INTERCHAIN EXCITATIONS

As described in the previous section, the properties of the interchain excited state wave functions determine the strength of the ISC rates. In this section we investigate such states. We use the term interchain excitations to describe excitations that are predominately composed of Coulombically bound interchain particle-hole excitations. (Here, we generally make no distinction between "polaron-pairs," "exciplexes," or "charge-transfer excitons," as such distinctions are not rigorous for general coupled systems.[22])

Since the Coulomb operator commutes with the number operator, Coulomb interactions preserve the charge on each chain. The Coulomb operator, therefore, cannot mix different components of interchain excitations, nor can it mix interchain excitations with intrachain excitations. We therefore conclude that in the absence of direct exchange, only interchain hopping processes can lift the singlet-triplet degeneracy. This is done by two ways: (1) mixing interchain excitations with doubly excited intrachain and ground state configurations, leading to kinetic exchange interactions; and (2) direct mixing between interchain and intrachain excitations. We now discuss each of these processes.

A. Kinetic exchange interactions

Kinetic exchange[26] raises the energy of the interchain singlet relative to the interchain triplet, provided that the repeat units are not perfectly co-facial. To see this consider the degenerate interchain $S_z=0$ basis states for a pair of dimers (illustrated in Fig. 1),

$$|A\rangle = \hat{a}^{\dagger}_{1-\uparrow}\hat{a}_{2+\uparrow}|GS\rangle \tag{14}$$

and

$$|B\rangle = \hat{a}^{\dagger}_{1-\downarrow}\hat{a}_{2+\downarrow}|GS\rangle \tag{15}$$

with energy $E_i = \Delta E + 3(\tilde{U}+\tilde{V})$, where $\hat{a}^{\dagger}_{n\pm\sigma}$ creates an electron with spin σ in the bonding (+) or antibonding (−) molecular orbital on dimer n.

The one-electron interchain Hamiltonian, $\hat{H}^{1e}_{\text{inter}}$, connects these states to the virtual doubly occupied state,

$$|1\rangle = \hat{a}^{\dagger}_{1-\uparrow}\hat{a}^{\dagger}_{1-\downarrow}\hat{a}_{2+\uparrow}\hat{a}_{2+\downarrow}|GS\rangle \tag{16}$$

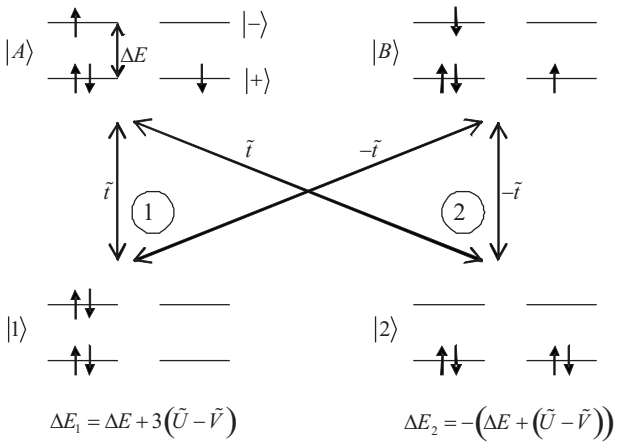

FIG. 1. The two virtual processes that mix the $S_z=0$ eigenstates $|A\rangle$ and $|B\rangle$ to form definite spin eigenstates. Process 2, connecting $|A\rangle$ and $|B\rangle$ to $|2\rangle$, dominates giving an effective positive exchange interaction that raises the energy of the singlet relative to the triplet.

with energy $E_1 = 2\Delta E + 6\tilde{U}$ and to the ground state, $|2\rangle \equiv |GS\rangle$, with energy $E_2 = 2\tilde{U} + 4\tilde{V}$. The parameters with tildes are molecular orbital parameters related to the atomic orbital parameters via $\tilde{U} = (V_0 + V_1)/2$ and $\tilde{V} = (2V_2 + V_3 + V_4)/4$, where V_j is the Ohno potential for neighboring sites, as shown in Fig. 2. The highest occupied molecular orbital–lowest unoccupied molecular orbital (HOMO-LUMO) energy gap is $\Delta E = 2t_1$.

Thus, the effective exchange interactions are

$$J_1 = -\frac{\tilde{t}^2}{(E_1 - E_i)} \tag{17}$$

and

$$J_2 = -\frac{\tilde{t}^2}{(E_2 - E_i)}, \tag{18}$$

where $\tilde{t} = (t_3 - t_4)/2$. The total kinetic exchange interaction is therefore

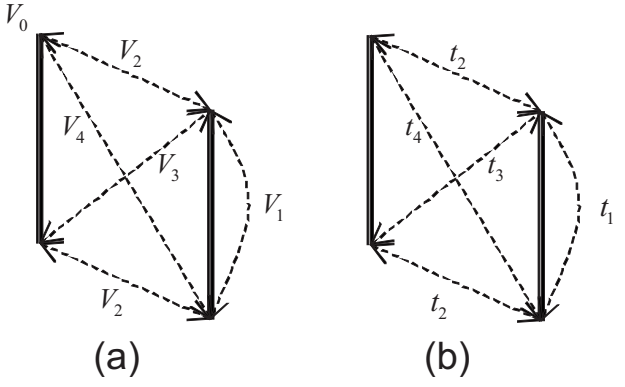

FIG. 2. Illustrating the Coulomb and hopping interactions between the two dimers.

$$J = J_1 + J_2 = \frac{2\tilde{t}^2(\tilde{U} - \tilde{V})}{[\Delta E + 3(\tilde{U} - \tilde{V})][\Delta E + (\tilde{U} - \tilde{V})]}. \quad (19)$$

Notice that $J>0$ because process "2" (illustrated in Fig. 1) dominates.

The Hamiltonian matrix for kinetic exchange in the basis $\{|A\rangle, |B\rangle\}$ is

$$\begin{pmatrix} J & -J \\ -J & J \end{pmatrix}, \quad (20)$$

with eigenstates

$$|S=1;\ S_z=0\rangle = \frac{1}{\sqrt{2}}(|A\rangle + |B\rangle) \quad (21)$$

at $E_T=0$, and

$$|S=0\rangle = \frac{1}{\sqrt{2}}(|A\rangle - |B\rangle) \quad (22)$$

at $E_S=2J$. The kinetic exchange gap is therefore $2J$ and vanishes for co-facial dimers, as then $t_3=t_4$ and $\tilde{t}=0$.

This result may be understood physically as follows. First, the triplet state is unperturbed by kinetic exchange, as may be seen by considering the $S_z=1$ component, whose parallel spins are forbidden by the Pauli principle to occupy the same orbital. Second, the singlet state is "repelled" by the higher and lower states, $|1\rangle$ and $|2\rangle$, respectively. However, since $|\Delta E_2| < |\Delta E_1|$, the repulsion from the ground state dominates, and the energy of the interchain state is raised.[28]

The second-order perturbation in the singlet energy implies a first-order perturbation in its wave function, and thus to leading order the difference between the singlet and triplet interchain wave functions is proportional to $\tilde{t}/\Delta E$. As described in Sec. II C, this implies that the spin-orbit coupling matrix elements between these states is also proportional to $\tilde{t}/\Delta E$, and becomes vanishing for weak intermolecular interactions. (In addition to this indirect kinetic exchange mechanism, there is also of course direct exchange arising from the Coulomb repulsion of the wave function overlap. This also lowers the energy of the triplet relative to the singlet.)

B. Intrachain and interchain exciton mixing

As well as processes 1 and 2 illustrated in Fig. 1 that exchange electron spins, the intermolecular hopping mixes

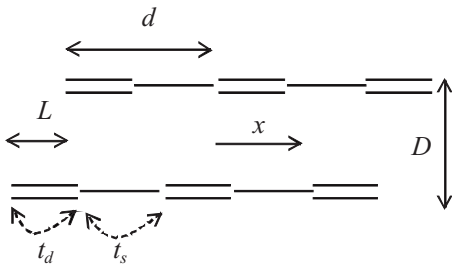

FIG. 3. The spatial geometries and parameters used in the model calculations 1 and 2. In both cases $t_d=-3.0$ eV, $t_s=-2.0$ eV, $d=2.8$ Å, and $D=4.0$ Å.

TABLE I. Parameters defined in Fig. 3 used in the model calculations. The hybridization integrals are determined by assuming that they are proportional to the wave function overlap, evaluated using Slater orbitals, and normalized with respect to the $C-C$ hybridization integral (taken to be 2.5 eV). In both cases $t_d=-3.0$ eV, $t_s=-2.0$ eV, $U=8$ eV, $\epsilon=2$, and the interchain distance, $D=4$ Å. L is the relative longitudinal displacement of the chains.

Parameters	Calculation 1:D_2 symmetry	Calculation 2:C_2 symmetry
L (Å)	0	0.7
t_2 (eV)	0.058	0.055
t_3 (eV)	0	0.039
t_4 (eV)	0	0.020

interchain and intrachain excitations. To second order in perturbation theory this leads to a correction in energy of $\tilde{t}^2/\Delta E$, where ΔE is the difference in energies between the interchain and intrachain excitations. The sign in the shift in energies arising from this mixing is determined by the energetic proximity of nearby states.

C. Model calculations

As the discussions in the previous sections illustrates, the differences between the singlet and triplet interchain excited state wave functions arise from high-order (i.e., two-particle) processes. Such processes require a rigorous approach to electron correlation (and lie outside the scope of CI-singles calculations). In this section we apply the density matrix renormalization group (DMRG) method[27] to solve the Pariser-Parr-Pople model for models systems that are parametrized to describe phenyl-based systems.

The model calculations for linear polyenes are calculations 1 and 2 described in Sec. II B. The geometry of the coupled chains is illustrated in Fig. 3, while the relevant parameter sets are shown in Table I. In the next section we briefly review the Pariser-Parr-Pople model, before describing the results. Relevant technical details of the DMRG method and convergence tests are described in the Appendix.

1. Pariser-Parr-Pople model

The Pariser-Parr-Pople (or extended Hubbard) model is a π-electron model of conjugated polymers, defined by

TABLE II. Low-energy excitations for 6 sites. $t_d=-3.0$ eV, $t_s=-2.0$ eV, $U=8$ eV, and $\epsilon_r=2$.

State	Energy (eV)	Quantum number, n	Quantum number, j
$1\ ^3B_u^+$	3.176	1	1
$1\ ^3A_g^+$	4.197	1	2
$2\ ^3B_u^+$	4.958	1	3
$1\ ^1B_u^-$	5.501	1	1
$2\ ^1A_g^+$	5.834	2	1
$1\ ^3A_g^-$	7.703	2	1

TABLE III. Low-energy singlet excitations for 2×6 sites for Calculation 1 (defined by Fig. 3 and Table I).

State	Energy (eV)	$\sigma(xy)$	$\sigma(yz)$	Particle-hole	Quantum number, n	Type
1	5.378	−1	−1	−1	1	Intra
2	5.597	+1	−1	−1	1	Intra
3	5.827	−1	+1	+1	2	Intra
4	5.830	+1	+1	+1	2	Intra
5	6.056	+1	−1	+1	1	Inter
6	6.074	−1	−1	−1	1	Inter

$$\hat{H} = -\sum_{ij\sigma} t_{ij}(\hat{c}^{\dagger}_{i\sigma}\hat{c}_{j\sigma} + \hat{c}^{\dagger}_{j\sigma}\hat{c}_{i\sigma}), \tag{23}$$

$$+ U\sum_{i}(\hat{N}_{i\uparrow} - 1/2)(\hat{N}_{i\downarrow} - 1/2) + \frac{1}{2}\sum_{i\neq j} V_{ij}(\hat{N}_i - 1)(\hat{N}_j - 1), \tag{24}$$

where $\hat{c}^{\dagger}_{i\sigma}$ creates a π electron on site i, $\hat{N}_{i\sigma}=\hat{c}^{\dagger}_{i\sigma}\hat{c}_{i\sigma}$, and $\hat{N}_i = \hat{N}_{i\uparrow}+\hat{N}_{i\downarrow}$.

We use the Ohno parameterization for the Coulomb interaction, defined by

$$V_{ij} = U/\sqrt{1 + (U\epsilon_r r_{ij}/14.397)^2}, \tag{25}$$

where r_{ij} is the interatomic distance (in Å), U is the on-site Coulomb interaction (in eV), and ϵ_r is the relative permittivity. This interaction is an interpolation between an on-site Coulomb repulsion, U, and a Coulomb potential, $e^2/4\pi\epsilon\epsilon_0 r_{ij}$ as $r_{ij}\rightarrow\infty$. We use the screened parameter set derived by Chandross and Mazumdar[29] to account for solvation effects. These parameters are $U=8$ eV and $\epsilon_r=2$.

2. Single chain results

The lowest energy excitations for a single linear chain of six sites is shown in Table II for model parameters that approximately parametrize poly(para-phenylene). The states are labeled by the principle and pseudomomentum exciton quantum numbers, n and j, respectively.[30–32] We note that for six sites there are three triplet excitons below the lowest singlet exciton, and that the $n=2$ singlet exciton lies lower in energy than the $n=2$ triplet exciton.

3. Coupled chain results

We first consider coupled chains with high spatial symmetry (calculation 1). Table III shows the exact low-energy singlet spectrum for two linear aligned chains of six sites each. There are two sets of predominately intrachain excitons lying below the first set of predominately interchain excitations. The former are formed from bonding and antibonding combinations of the $n=1$ and $n=2$ intrachain singlet excitons. The lowest interchain excitation is predominately a polaron pair.[23] The higher-lying interchain excitation (state 6) is, however, mixed with the lowest-lying singlet exciton, and is thus an exciplex.

Table IV shows the corresponding triplet spectrum. As expected from the single-chain spectrum, there are three pairs of predominately intrachain excitons (all arising from the $n=1$ family) that lie below the interchain excitations. The lowest triplet interchain excitation is essentially degenerate with its singlet counterpart.[33] For this high symmetry system the matrix elements of the spin-orbit coupling operator between the interchain excitations vanish by symmetry, so we no longer consider it.

Tables V and VI show the low-energy spectrum for coupled chains with lower spatial symmetry, in particular linear chains displaced by 0.7 Å, so that the overall system

TABLE IV. Low-energy triplet excitations for 2×6 sites for Calculation 1 (defined by Fig. 3 and Table I).

State	Energy (eV)	$\sigma(xy)$	$\sigma(yz)$	Particle-hole	Quantum number, n	Type
1	3.172	−1	−1	+1	1	Intra
2	3.176	+1	−1	+1	1	Intra
3	4.193	−1	+1	+1	1	Intra
4	4.197	+1	+1	+1	1	Intra
5	4.956	−1	−1	+1	1	Intra
6	4.959	+1	−1	+1	1	Intra
7	6.056	+1	−1	−1	1	Inter
8	6.059	−1	−1	+1	1	Inter

TABLE V. Low-energy singlet excitations for 2×6 sites for Calculation 2 (defined by Fig. 3 and Table I).

State	Energy (eV)	C_2	Quantum number, n	Type
1	5.383	+1	1	Intra
2	5.592	−1	1	Intra
3	5.827	−1	2	Intra
4	5.829	+1	2	Intra
5	6.063	−1	1	Inter
6	6.076	+1	1	Inter

has C_2 symmetry (calculation 2). We also include next-nearest-neighbor interchain hopping, so that the particle-hole symmetry is lifted. Now the lowest interchain excitations mix with the lower intrachain excitons. They also experience kinetic exchange, as described in Sec. III A, because $t_3 \neq t_4$, and thus the triplet interchain excitation lies slightly lower in energy than the singlet.

4. Spin-orbit coupling matrix elements

We now consider matrix elements of the dimensionless spin-orbit coupling operator

$$\hat{O}_{SO} = \sum_{n}^{N-1} (\hat{c}^{\dagger}_{n\uparrow}\hat{c}_{n+1\downarrow} - \hat{c}^{\dagger}_{n+1\uparrow}\hat{c}_{n\downarrow}) \tag{26}$$

between the triplet and singlet interchain excitations with opposite inversion symmetry, i.e.,

$$\langle \hat{O}_{SO} \rangle \equiv \langle S=1,\ S_z=1;\ C_2=-1|\hat{O}_{SO}|S=0;\ C_2=+1\rangle. \tag{27}$$

These matrix elements, with the corresponding energy gap, $\Delta E_{TS} \equiv E(S=1,\ S_z=1;\ C_2=-1) - E(S=0,\ C_2=+1)$, are calculated by the DMRG method and shown in Table VII. Since the spectrum of intrachain excitations below the lowest interchain excitation becomes denser as the chain length increases, results to our desired accuracy (namely ca. 0.001 eV in the excitation energies and ca. 20% in the matrix elements) are only possible for chains of up to 12 sites. However, since the effective conjugation length in light-emitting polymers is ca. 8–10 repeat units,[34] these results are expected to be relevant for realistic systems. (Full DMRG convergence tables are shown in the Appendix.)

TABLE VI. Low-energy triplet excitations for 2×6 sites for Calculation 2 (defined by Fig. 3 and Table I).

State	Energy (eV)	C_2	Quantum number, n	Type
1	3.173	+1	1	Intra
2	3.176	−1	1	Intra
3	4.194	−1	1	Intra
4	4.196	+1	1	Intra
5	4.956	+1	1	Intra
6	4.958	−1	1	Intra
7	6.061	−1	1	Inter
8	6.064	+1	1	Inter

TABLE VII. Triplet-singlet energy splitting and spin-orbit coupling matrix elements for Calculation 2 (defined by Fig. 3 and Table I).

Number of sites per chain	ΔE_{TS} (eV)	$\langle \hat{O}_{SO} \rangle \times 10^{-4}$
4	−0.013	5.0
6	−0.016	1.9
8	−0.017	5.2
10	−0.017	7.7
12	−0.017	10.9

We note that the triplet lies energetically below the singlet, with the energy gap between them being less than k_BT, in agreement with previous work.[24] (Note, the energy difference between the triplets and singlets with the same spatial symmetry is even smaller, being typically 2 meV.) We also see that the spin-orbit coupling matrix elements between these interchain states are very small, being essentially 10^3-10^4 times smaller than the corresponding matrix elements between intramolecular states. The numerical value of the spin-orbit coupling is $\langle \hat{H}_{SO} \rangle = A\langle \hat{O}_{SO} \rangle$, where $A=B \sin\theta$ and $|B|=3.94\times10^{-4}$ eV. Thus, $|\langle \hat{H}_{SO} \rangle|$ ca. 1×10^{-7} eV, taking $\theta=20°$.

IV. DISCUSSION AND CONCLUSIONS

Using theoretical arguments we have shown that spin-orbit coupling between Coulombically bound interchain excitations in conjugated polymers is vanishing for ideal systems and negligible for realistic systems. As well as the usual reasons for why spin-orbit coupling is small in π-conjugated polymers, we have shown that it is particularly small between low-lying interchain excitations, because these states have wave functions that differ by an amount proportional to the interchain one-electron hopping integral, t_{inter}, which vanishes as the intermolecular interactions vanish.

Using DMRG calculations on model systems we confirm these theoretical predictions: spin-orbit coupling between interchain states is typically 10^3-10^4 times smaller than between corresponding intrachains states, being ca. 1×10^{-7} eV for the parameter sets considered in this paper. Since the spin-orbit coupling is proportional to t_{inter}, reducing the interchain separation will increase the coupling, but it will always be negligible for realistic values of t_{inter}. (Note, however, we predict that spin-orbit coupling vanishes for perfectly co-facial polymers.)

We have also performed *ab initio* calculations of the excitation energies and spin-orbit coupling for coupled biphenyl molecules using the CIS(D)[35] method including two-electron spin-orbit coupling. These results, which confirm our model calculations, will be presented shortly.[36]

TABLE VIII. Convergence results for the DMRG calculations for various convergence parameters for Calculation 2 (defined by Fig. 3 and Table I). Number of sites per chain, N; superblock Hilbert space size, SBHSS; ground state energy, E_{GS}, in eV; excitation energy of the singlet interchain excitation $|S=0;\ C_2=+1\rangle$, ΔE_{SS}, in eV.

	Run 1			Run 2			Run 3		
N	SBHSS	E_{GS}	ΔE_{SS}	SBHSS	E_{GS}	ΔE_{SS}	SBHSS	E_{GS}	ΔE_{SS}
4	Exact	−34.8012	7.059	Exact	−34.8012	7.059	Exact	−34.8012	7.059
6	Exact	−52.7670	6.076	Exact	−52.7670	6.076	Exact	−52.7670	6.076
8	0.99×10^6	−70.7339	5.549	2.93×10^6	−70.7386	5.544	6.55×10^6	−70.7389	5.543
10	0.69×10^6	−88.6969	5.244	3.05×10^6	−88.7108	5.228	5.72×10^6	−88.7117	5.226
12	0.92×10^6	−106.6564	5.078	2.76×10^6	−106.6814	5.030	5.67×10^6	−106.6840	5.024

We have shown that spin-orbit coupling vanishes for highly symmetric arrangements of polymers. For these systems it is possible for electron-phonon coupling to induce a symmetry-allowed transition. However, the matrix elements will still be vanishingly small for the same reasons that they are for lower-symmetry systems, namely the near degeneracy of the interchain excitations. The addition of heteroatoms may also weakly change our conclusions, but again so long as the polymers are equivalent, the near degeneracy of the interchain excitations will ensure small spin-orbit coupling matrix elements.

The work described here is motivated by a desire to find a mechanism for the possible enhanced singlet exciton yield in light-emitting polymers. As described in Sec. I, such a mechanism (if it exists) relies on an intersystem crossing rate being comparable to or faster than the interconversion rate from the interchain to intrachain triplet states. According to Ref. 15 these interconversion rates are predominately determined by the overlap of the vibrational wave functions of the initial and final states. Assuming that interconversion only occurs between the lowest interchain state and the lowest pseudomomentum component of the intramolecular state (which is only true provided that selection rules appropriate to well-ordered chains hold), then the one-electron interconversion matrix element is

$$\langle \hat{H}_{\text{inter}} \rangle \sim t_{\text{inter}} \left(\frac{\exp(-S) S^{\nu}}{\nu!} \right)^{1/2}. \tag{28}$$

Typically for light-emitting polymers $\nu_T \simeq 8$, $\nu_S \simeq 4$, and $S \sim 0.5$. Using $t_{\text{inter}}=0.05$ eV gives $\langle \hat{H}_{\text{inter}} \rangle_T \simeq 1\times10^{-5}$ eV and $\langle \hat{H}_{\text{inter}} \rangle_S \simeq 2\times10^{-3}$ eV for triplet and singlet interconversion, respectively. Bearing in mind that these results are underestimates of the interconversion matrix elements, we see that an ISC rate arising from spin-orbit coupling cannot compete with interconversion rates. This conclusion is in agreement with the experimental observations of Reufer *et al.*,[16,37] who reported ISC rates of $\ll 10^5$ s^{-1} between Coulombically bound interchain excitations. This observation contrasts with reported ISC rates between exciplexes across a heterojunction of $>2\times10^6$ s^{-1} by Ford *et al.*[38] However, since exciplexes at a heterojunction are linear combinations of polaron pairs and intramolecular excitons, it is unclear how relevant this value is for interchain excitations at a regular junction.

The question then remains: What, if any, ISC mechanism competes with interconversion processes? Since the interchain excitations are weakly bound, scattering of these pairs with free charge carriers will cause ISC, preferentially from triplet to singlets because the triplets are longer lived. However, modeling this process is complicated by the particular device characteristics which determine local charge imbalances. Without such modeling it is unclear whether this ISC mechanism is able to compete with interconversion processes.[39]

ACKNOWLEDGMENTS

This work was supported by the EPSRC (U.K.) (Grant No. EP/D038553/1) and the John Fell Fund of the University of Oxford. We thank M. C. Gibson for useful discussions.

APPENDIX: DETAILS OF THE DMRG CALCULATIONS

The interchain or intrachain character of the excited states is determined by measuring the particle-hole excitation weights,[31,40] defined via the singlet or triplet particle-hole excitation operator,

$$^{1}_{3}\hat{O}_{mn} = \frac{1}{\sqrt{2}} (\hat{a}^{\dagger}_{m-\uparrow} \hat{a}_{n+\uparrow} \pm \hat{a}^{\dagger}_{m-\downarrow} \hat{a}_{n+\downarrow}) \tag{A1}$$

where $\hat{a}^{\dagger}_{m\pm\sigma}$ creates an electron with spin σ in the bonding (+) or antibonding (−) molecular orbital on repeat unit m. The intrachain weight is

$$W_{\text{intra}} = \sum_{m\in1, n\in1} |\Psi_{mn}|^2 \tag{A2}$$

while the intrachain weight is

TABLE IX. Same as Table VIII, for Run 4.

	Run 4		
N	SBHSS	E_{GS}	ΔE_{SS}
4	Exact	−34.8012	7.059
6	Exact	−52.7670	6.076
8	12.43×10^6	−70.7389	5.543
10	10.83×10^6	−88.7120	5.225
12	10.80×10^6	−106.6853	5.023

TABLE X. Convergence results for the DMRG calculations for various convergence parameters for Calculation 2 (defined by Fig. 3 and Table I). Number of sites per chain, N; energy gap between the triplet and singlet interchain excitations, $\Delta E_{TS}=E(S=1,\ S_z=1;\ C_2=-1)-E(S=0;\ C_2=+1)$ in eV; spin-orbit coupling matrix element $\langle\hat{O}_{SO}\rangle=\langle S=1,\ S_z=1;\ C_2=-1|\hat{O}_{SO}|S=0;\ C_2=+1\rangle$, with $\hat{O}_{SO}$ defined in Eq. (27). The results for four and six sites per chain are exact.

	Run 1		Run 2		Run 3	
N	ΔE_{TS}	$\langle\hat{O}_{SO}\rangle\times 10^{-4}$	ΔE_{TS}	$\langle\hat{O}_{SO}\rangle\times 10^{-4}$	ΔE_{TS}	$\langle\hat{O}_{SO}\rangle\times 10^{-4}$
4	−0.013	5.0	−0.013	5.0	−0.013	5.0
6	−0.016	1.9	−0.016	1.9	−0.016	1.9
8	−0.018	4.4	−0.016	4.9	−0.017	5.2
10	−0.016	6.5	−0.016	6.3	−0.017	7.7

$$W_{\text{inter}}=\sum_{m\in 1,n\in 2}|\Psi_{mn}|^2, \tag{A3}$$

where

$$\Psi_{mn}=\langle\Psi|\hat{O}_{mn}|GS\rangle, \tag{A4}$$

and $|GS\rangle$ and $|\Psi\rangle$ are the ground state and excited state, respectively.

In our DMRG algorithm we employ the sparse symmetry operator techniques for computing symmetry adapted eigenstates described in Ref. 41. This approach allows us to target eigenstates with specific spin-flip, particle-hole, and reflection (short and long axis in the case of coupled chains) symmetries by expressing the DMRG superblock symmetry operators as tensor products of operators from the individual blocks that make up the superblock (in the case of the present model, a system block, a reflected system block, and two added repeat units in the middle). The block symmetry operators can be kept sparse throughout the course of the DMRG algorithm by exploiting the fact that the operators obey a type of commutativity with the reduced density matrix, whose eigenstates are used to form new block bases when the system blocks are augmented by adding one of the middle blocks. The generalized commutativity relation implies that the augmented block symmetry operators are sparse in this new rotated basis—a result of the fact that the density matrix eigenstates must be eigenstates of the symmetry operators or are connected to precisely one other density matrix eigenstate in a different z-spin-charge $(Q,\ S^z)$ subspace. For example, in the case of the spin-flip operator $\hat{P}$, in subspaces where $S^z=0$, the density matrix eigenstates are eigenstates of the spin-flip operator, *viz*

$$\hat{P}|Q,0,n\rangle^{(a')}=p(Q,0,n)|Q,0,n\rangle^{(a')},$$

where $|Q,S^z,n\rangle^{(a')}$ denotes the nth density matrix eigenstate, or rotated augmented block basis state, in the (Q,S^z) z-spin-charge sector, and $p(Q,0,n)\in\{+1,-1\}$ is the eigenvalue of the spin-flip operator. For the other subspaces (where $S^z\neq 0$), we can fix the arbitrary phase factors in the density matrix eigenstates in the $S^z<0$ sectors so that the spin-flip operator satisfies the general sparsity relation

$$\hat{P}|Q,S^z,n\rangle^{(a')}=p(Q,S^z,n)|Q,-S^z,n\rangle^{(a')}, \tag{A5}$$

with $p(Q,S^z,n)\equiv 1$ for all $S^z\neq 0$.

The derivation of this result, presented in the appendix of Ref. 41, assumed that all superblock target states making up the Gibbs state projection operator that is partially traced to form the reduced (augmented block) density matrix have total $S^z_s=0$ (these can be singlets or $S^z_s=0$ branches of triplet excitations). It was mentioned that it is possible to generalize the Gibbs states to include target states with nonzero superblock z spin. Indeed, this is required for the calculations in this paper, as we need to compute matrix elements between superblock eigenstates with $S^z_s=0$ and those with $S^z_s=1$ (the branches of the low-lying triplet excitations with $S^z_s=1$). This can be achieved by ensuring that for each $S^z_s=1$ target state we compute and add into the Gibbs state, we compute the corresponding $S^z_s=-1$ state and add it in also to the Gibbs state, with the same weight factor. In fact, once we have computed $S^z_s=1$ states, we do not need to compute the corresponding $S^z_s=-1$ by superblock Hamiltonian diagonalization. Rather, we can simply apply the superblock spin-flip operator to the $S^z_s=1$ state and this will generate the corresponding $S^z_s=-1$ state. A further efficiency can be obtained by simply forming the asymmetric Gibbs state containing just the $S^z_s=0$ and $S^z_s=1$ states required for our spin-orbit calculations, forming the corresponding reduced density matrix (which will not satisfy the generalized commutativity relation), and then symmetrizing it. That is, if $\hat{\rho}(S^z)$ denotes the reduced density matrix in the subspace with z spin S^z, then we replace $\rho(\hat{S}^z)$ with

$$\hat{\rho}'(S^z)\equiv\frac{1}{2}(\hat{\rho}(S^z)+\hat{P}\hat{\rho}(-S^z)\hat{P})$$

This new symmetrized density matrix is then guaranteed to satisfy the generalized commutativity relation

$$\hat{\rho}'(S^z)=\hat{P}\hat{\rho}'(-S^z)\hat{P}$$

required to establish the sparsity condition (A5) of the rotated augmented block spin-flip operator. Indeed this approach is equivalent to adding in the $S^z_s=-1$ states to the Gibbs state (and directly deriving a symmetric density

matrix) as long as the weights of the $S_s^z=0$ states are divided by 2 relative to $S_s^z=1$ states in the asymmetric Gibbs state.

Tables VIII–X show the convergence of the excitation energies and spin-orbit coupling matrix elements. For the convergence parameters used in the results described in Sec. III C, namely Run 3, we see that the excitation energies have converged to ca. 0.001 eV, which is considerably smaller than the singlet-triplet interchain exchange splitting. Spin-orbit coupling matrix elements have converged to better than 20%.

*william.barford@chem.ox.ac.uk
†robert.bursill@unsw.edu.au
‡dmitry.makhov@chem.ox.ac.uk

[1] Y. Cao, I. D. Parker, G. Yu, C. Zhang, and A. J. Heeger, Nature (London) **397**, 414 (1999).
[2] P. K. H. Ho, J.-S. Kim, J. H. Burroughes, H. Becker, F. Y. L. Sam, T. M. Brown, F. Cacialli, and F. H. Friend, Nature (London) **404**, 481 (2000).
[3] J. S. Wilson, A. S. Dhoot, A. J. A. B. Seeley, M. S. Khan, A. Köhler, and R. H. Friend, Nature (London) **413**, 828 (2001).
[4] M. Wohlgenannt, K. Tandon, S. Mazumdar, S. Ramasesha, and Z. V. Vardeny, Nature (London) **409**, 494 (2001).
[5] M. Wohlgenannt, X. M. Jiang, Z. V. Vardeny, and R. A. J. Janssen, Phys. Rev. Lett. **88**, 197401 (2002).
[6] M. Wohlgenannt, C. Yang, and Z. V. Vardeny, Phys. Rev. B **66**, 241201(R) (2002).
[7] A. S. Dhoot, D. S. Ginger, D. Beljonne, Z. Shuai, and N. C. Greenham, Chem. Phys. Lett. **360**, 195 (2002).
[8] M. Segal, M. A. Baldo, R. J. Holmes, S. R. Forrest, and Z. G. Soos, Phys. Rev. B **68**, 075211 (2003).
[9] M. N. Kobrak and E. R. Bittner, Phys. Rev. B **62**, 11473 (2000).
[10] S. Karabunarliev and E. R. Bittner, Phys. Rev. Lett. **90**, 057402 (2003); J. Chem. Phys. **119**, 3988 (2003).
[11] T.-M. Hong and H.-F. Meng, Phys. Rev. B **63**, 075206 (2001).
[12] Z. Shuai, D. Beljonne, R. J. Silbey, and J. L. Brédas, Phys. Rev. Lett. **84**, 131 (2000).
[13] A. Ye, Z. Shuai, and J. L. Brédas, Phys. Rev. B **65**, 045208 (2002).
[14] K. Tandon, S. Ramasesha, and S. Mazumdar, Phys. Rev. B **67**, 045109 (2003).
[15] W. Barford, Phys. Rev. B **70**, 205204 (2004).
[16] M. Reufer, M. J. Walter, P. G. Lagoudakis, A. B. Hummel, J. S. Kolb, H. G. Roskos, U. Scherf, and J. M. Lupton, Nat. Mater. **4**, 340 (2005).
[17] M. A. El-Sayed, J. Chem. Phys. **38**, 2834 (1963).
[18] K. Schmidt, S. Brovelli, V. Coropceanu, D. Beljonne, J. Cornil, C. Bazzani, T. Caronna, R. Tubino, F. Meinardi, Z. Shuai, and J. L. Brédas, J. Phys. Chem. A **111**, 10490 (2007).
[19] D. Beljonne, Z. Shuai, G. Pourtois, and J. L. Brédas, J. Phys. Chem. A **105**, 3899 (2001).
[20] J. Rybicki and M. Wohlgenannt, Phys. Rev. B **79**, 153202 (2009).
[21] M. C. Gibson (unpublished).
[22] Interchain excitations have been considered by Mazumdar and co-workers in the context of photoinduced absorption (Ref. 23), and Refs. 24 and 25 in the context of electron-hole recombination.
[23] Z. Wang, S. Mazumdar, and A. Shukla, Phys. Rev. B **78**, 235109 (2008); D. Psiachos and S. Mazumdar, *ibid.* **79**, 155106 (2009).
[24] A. Kadashchuk, A. Vakhnin, I. Blonski, D. Beljonne, Z. Shuai, J. L. Brédas, V. I. Arkhipov, P. Heremans, E. V. Emelianova, and H. Bässler, Phys. Rev. Lett. **93**, 066803 (2004).
[25] S. Difley, D. Beljonne, and T. van Voorhis, J. Am. Chem. Soc. **130**, 3420 (2008).
[26] P. W. Anderson, Phys. Rev. **115**, 2 (1959).
[27] S. R. White, Phys. Rev. Lett. **69**, 2863 (1992).
[28] Our conclusion is opposite to that of Ref. 25 who predicted that kinetic exchange stabilizes the singlet interchain excitation.
[29] M. Chandross and S. Mazumdar, Phys. Rev. B **55**, 1497 (1997).
[30] W. Barford, R. J. Bursill, and R. W. Smith, Phys. Rev. B **66**, 115205 (2002).
[31] W. Barford and N. Paiboonvorachat, J. Chem. Phys. **129**, 164716 (2008).
[32] W. Barford, *Electronic and Optical Properties of Conjugated Polymers* (Oxford University Press, Oxford, 2005).
[33] To higher precision, the excitation energies of the lowest singlet and triplet interchain states are 6.055966 and 6.056037 eV, respectively.
[34] W. Barford and D. Trembath, Phys. Rev. B **80**, 165418 (2009).
[35] M. Head-Gordon, R. A. Rico, M. Oumi, and T. J. Lee, Chem. Phys. Lett. **219**, 21 (1994).
[36] D. V. Makhov and W. Barford (unpublished).
[37] Note, however, that the explanation given in Ref. 16 for the negligible spin-orbit coupling between interchain singlet and triplet excitations, namely, a sizeable exchange interaction between these states, is precisely the opposite of the correct explanation, namely, a vanishing exchange interaction, and hence similar wave functions.
[38] T. A. Ford, H. Ohkita, S. Cook, J. R. Durrant, and N. C. Greenham, Chem. Phys. Lett. **454**, 237 (2008).
[39] Hyperfine interactions are sometimes cited as a possible cause of intersystem crossing in conjugated polymers. However, as the nucleus of ^{12}C possess no magnetic dipole moment, the only possible hyperfine interaction involving π electrons is with their electric field gradients and the electric-quadrupole moment of the ^{12}C nuclei.
[40] W. Barford, R. J. Bursill, and M. Yu Lavrentiev, J. Phys.: Condens. Matter **10**, 6429 (1998).
[41] R. J. Bursill and W. Barford, J. Chem. Phys. **130**, 234302 (2009).